Journal of Sound and Vibration (2000) **234**(1), 21–42
doi:10.1006/jsvi.1999.2857, available online at http://www.idealibrary.com on IDEAL®

PHASE VELOCITY OF RUBBER ELEMENT IN VIBRATION ISOLATOR UNDER STATIC LOAD

J. D. Dickens

Defence Science and Technology Organisation (DSTO), Aeronautical and Maritime Research Laboratory (AMRL), P.O. Box 4331, *Melbourne, Victoria* 3001, *Australia*

(*Received* 14 *April* 1999, *and in final form* 26 *November* 1999)

The dynamic properties of the rubber element of a vibration isolator are affected by its compression ratio, and thus the dynamic characteristics of a vibration isolator depend upon the static load. A vibration isolator may be modelled in terms of its phase velocity. Therefore, to predict the effect of the static load, a knowledge of the relationship between the phase velocity of the rubber element and its compression ratio is required. This study proposes such a relationship, and applies it to experimental data from the literature. The proposed relationship is experimentally investigated and improved in a companion publication.

1. INTRODUCTION

The dynamic properties of a rubber are affected by its static compression. Thus, to assist in the development of vibration isolators, it is necessary to have a dynamic model of the vibration isolator that includes the effect of static compression. A model is required that predicts the dependence of the dynamic characteristics of a vibration isolator on its compression ratio. The compression ratio of a vibration isolator is defined as the static compressed height of the rubber element under load, divided by its uncompressed height. Thus, the compression ratio of an unloaded vibration isolator is unity. Snowdon [1] developed a model of a vibration isolator in terms of its four-pole parameters, which required the phase velocity of the rubber element. It is therefore necessary to know the dependence of the phase velocity on the compression ratio.

The vibration isolator is considered to comprise a resilient element of homogeneous rubber that is securely bonded to two end plates. The undeformed rubber element is assumed to have a regular right prismatic shape. Because rubber may be considered as incompressible, a practical vibration isolator under static compression produces deformation of the rubber element, which may be described as barrelling. Under deformation, the rubber element is assumed to have a regular right barrel shape with parallel ends. The end plates are used for attaching the vibration isolator to the upper and lower structures, and are assumed to have no structural modes in or near the frequency of interest. A rubber that is commonly used in vibration isolators is natural rubber vulcanisate with carbon black filler, and this study is concerned with this type of rubber.

Pure longitudinal waves cannot exist in a rod, because its lateral surfaces are free of constraints, thus permitting longitudinal stress to produce lateral strains via the Poisson ratio effect [2]. However, the quasi-longitudinal waves that exist will be referred to as longitudinal waves, in keeping with many other authors. It is assumed that plain cross-sections of the rod stay plain.

0022-460X/00/260021 + 22 $35.00/0

The barrelling behaviour is modelled by following a number of steps. Initially, the compressed rubber element is treated as a uniform rod that is a regular right prism, and the familiar longitudinal wave equation is used to model its behaviour. Longitudinal wave equations for rods have been derived [3]. The terms "bar" and "beam" are also used by other authors for the word "rod". The longitudinal wave equation for the compressed rubber element is derived, initially by treating it as a short rod with radial motion effects, and then by including the effect of the deformation on the apparent rubber properties. The short compressed rubber rod is then considered to have a barrel shape, and finally an equation is proposed for its phase velocity. This analysis is focused towards a cylindrical rod, which is a fundamental shape in modelling.

Complex numbers are represented with the superscript *, and real numbers are not superscripted. Imaginary components are represented using $\mathrm{j} = \sqrt{-1}$. In the contemporary literature, the commonly used symbols for the compression ratio and wavelength are both lambda, λ. Other authors have used the capital lambda symbol Λ for the wavelength. This study denotes the compression ratio and wavelength by the symbols λ and Λ respectively.

2. LONG RUBBER ROD

A long rod is defined to be a rod that has small lateral dimensions compared to the longitudinal wavelength. In this case, the radial motions caused by the longitudinal vibrations may be treated as negligible. It is assumed that the only stresses that occur are longitudinal in nature and are uniformly distributed across the cross-sections. Quantitatively, the lateral dimensions should be less than one-tenth of the wavelength [2].

Consider a long rubber rod that is homogeneous, of uniform cross-section and right prismatic shape. It has height h and cross-sectional area A, and is composed of a rubber having a dynamic complex normal modulus E_0^*, loss angle δ_0 and density ρ. Then the complex normal modulus for the long rod may be expressed as

$$E_0^* = E_0 \mathrm{e}^{\mathrm{j}\delta_0}. \tag{1}$$

From the wave equation the phase velocity for the undeformed rubber rod c_0^* is

$$c_0^* = \sqrt{\frac{E_0^*}{\rho}} \tag{2}$$

and from equation (1) this may be expressed as

$$c_0^* = c_0 \mathrm{e}^{\mathrm{j}\delta_0/2}. \tag{3}$$

The magnitude of the phase velocity for the undeformed rubber rod is $c_0 = |c_0^*|$. The internal dampening of the rod is taken into account by using complex numbers for E_0^* and c_0^*.

3. SHORT RUBBER ROD

A short rod is defined to be a rod which has lateral dimensions comparable to the longitudinal wavelength. This applies if the lateral dimensions are greater than one-tenth of the wavelength at the frequency of interest. Consider a short rubber rod that is

homogeneous, of uniform cross-section and right prismatic shape. Let the wavelength phase, velocity magnitude and frequency of the longitudinal wave in the short rubber rod be Λ_F, c_F and f respectively. Then

$$\omega = 2\pi f \tag{4}$$

and

$$c_F = f\Lambda_F. \tag{5}$$

Define the phase velocity reduction factor, Θ^*, as the ratio of the phase velocity of the short rubber rod c_F^* to that of the long rod, given by

$$\Theta^* = \frac{c_F^*}{c_0^*}. \tag{6}$$

Let the moment of inertia of a solid rod, of radius r and mass m, about its longitudinal axis be I. Then the radius of gyration r_G of the rod is defined by

$$I = r_G^2 m \tag{7}$$

which yields

$$r_G = \frac{r}{\sqrt{2}}. \tag{8}$$

For a short rod the radial motion that exists through the Poisson contraction cannot be ignored. For rubber, the loss angles for the complex elastic normal and shear moduli are assumed to be equal, and consequently the Poisson ratio v is a real number [4]. Love [5] developed a theory that considers this radial inertia by assuming that the radial displacement is proportional to the radius. This yields the phase velocity reduction factor as

$$\Theta^* = \left[1 - \left(\frac{\omega v r_G}{c_0^*}\right)^2\right]^{1/2}. \tag{9}$$

This approach for a short rod is also known as Rayleigh's correction for lateral inertia [3, 6]. Equation (9) may be re-arranged to give [5]

$$\Theta^* = \left[1 + \left(\frac{\omega v r_G}{c_F^*}\right)^2\right]^{-1/2}. \tag{10}$$

The magnitude of the phase velocity reduction factor is $\Theta = |\Theta^*|$. From equations (3) and (9) the phase velocity reduction factor may be expressed as

$$\Theta^* = \Theta e^{j\psi/2}, \tag{11}$$

where

$$\psi = \tan^{-1}\left[\frac{(\omega v r_G)^2 \sin\delta_0}{c_0^2 - (\omega v r_G)^2 \cos\delta_0}\right]. \tag{12}$$

3.1. ACCURACY OF PHASE VELOCITY REDUCTION FACTOR

Consider a short circular rod of radius r, length h and composed of a rubber having negligible loss factor. Therefore, $\delta_0 \cong 0$ which in equation (12) gives $\psi \cong 0$. With the

assumption that $v = 0{\cdot}5$, equations (4), (5), (8) and (10) imply

$$\Theta = \left[1 + \frac{\pi^2}{2}\left(\frac{r}{\Lambda_F}\right)^2\right]^{-1/2}. \tag{13}$$

The accuracy of the magnitude of the phase velocity reduction factor calculated from equation (13) may be compared with the exact solution determined by the Pochhammer–Chree theory [7, 8] for an infinitely long rod with various diameter-to-wavelength ratios. The exact theory has a dispersive solution with an infinite number of branches. In the current analysis, low frequencies are of concern and the mode of most interest is the first (symmetrical) one, referred to as the $M_{1,1}$ mode by Redwood [9]. The exact first mode values of the ratio of phase velocities, for a Poisson ratio of 0·5, agree closely with the ratios given by Davey and Payne [10] for rubber cylinders having diameter-to-wavelength ratios from 0·2 to 2. This first mode ratio is termed as phase velocity reduction factor for the exact Pochhammer–Chree solution.

The exact solution was evaluated using the following expression derived from the analysis by Bancroft [11] of the exact Pochhammer–Chree solution and simplified using $v = 0{\cdot}5$,

$$\frac{\mathrm{j}\pi X(3\Theta^2 - 2)^2\,\mathrm{J}_0(\mathrm{j}\pi X)}{4\mathrm{J}_1(\mathrm{j}\pi X)} + \frac{3\Theta^2}{2} - \pi X\sqrt{3\Theta^2 - 1}\,\frac{\mathrm{J}_0(\pi X\sqrt{3\Theta^2 - 1})}{\mathrm{J}_1(\pi X\sqrt{3\Theta^2 - 1})} = 0, \tag{14}$$

where $X = 2r/\Lambda_F$ is the diameter-to-wavelength ratio, J_0 is a Bessel function of the first kind of order 0, and J_1 is a Bessel function of the first kind of order 1.

The error of the phase velocity reduction factor for rubber using the Love theory, referenced to the exact solution, is shown in Figure 1. It does not exceed 4% for diameter-to-wavelength ratios from 0 to 1·20, and does not exceed 10% for diameter-to-wavelength ratios from 0 to 1·41. This analysis shows that Snowdon [4, p. 184] needs a minor correction to the statement that "the phase velocity predicted by the Love theory is never more than approximately 22% greater than that given by the exact theory" for diameter-to-wavelength ratios up to 2. These values in fact apply for a Poisson ratio of 0·29 applicable to steel [3], and not for rubber.

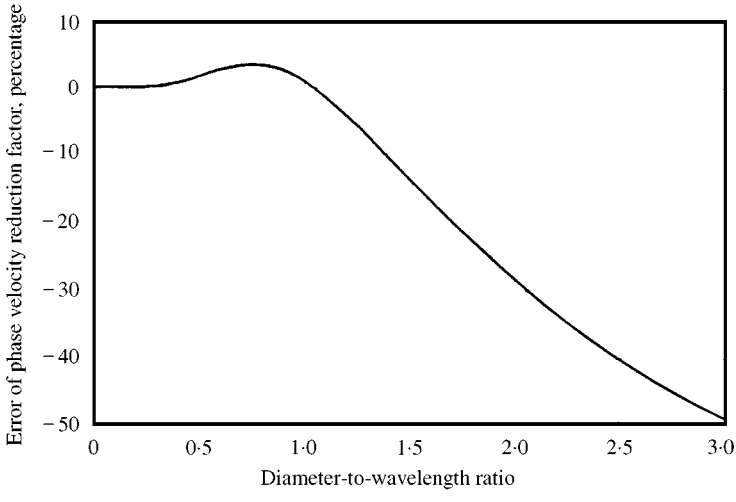

Figure 1. Magnitude error of phase velocity reduction factor for rubber, based on the Love theory.

4. EFFECT OF COMPRESSION RATIO ON RUBBER PROPERTIES

The rubber in a vibration isolator causes it to have non-linear behaviour. In common practice, the vibration isolator supports a machine and is subjected to a dynamic force superposed on a static load. Under normal operation, the input dynamic vibration amplitudes are generally much smaller than the compressed height of the rubber. The vibration isolator thus operates dynamically about a static point on its force displacement curve. For small dynamic strains of not greater than 1×10^{-3}, the complex normal modulus may be treated as constant [12, 13]. Under these conditions, the dynamic characteristics of a vibration isolator may be considered to be linear with respect to displacement, but still frequency dependent.

Consider the dynamic properties of a vibration isolator under a large static strain, i.e., larger than 10%. Since the shape factor depends only upon the geometry of the isolator and not the material properties, Payne [14] argued that it should have the same value for the real and imaginary components of the complex moduli. Payne [14–18] investigated the shape factors and functions for filled and unfilled rubber specimens under different static strains, and the major findings are presented by Payne [19]. He found that for a small sinusoidal strain superposed on a compression ratio λ, the dynamic elastic normal modulus E'_D of an unfilled rubber is related to its dynamic undeformed elastic shear modulus G'_0 by

$$E'_D = (1 + \beta S^2)\left(\frac{2 + \lambda^3}{\lambda^3}\right) G'_0, \tag{15}$$

where S is the shape factor of the undeformed rubber, and β is a constant.

This study uses the shape factor as defined by previous researchers [20, 21], i.e., the ratio of the loaded area at one end to the total force-free area of the undeformed rubber element. In the case of a cylindrical element of undeformed radius r_0 and undeformed height h_0, the shape factor is given by

$$S = \frac{r_0}{2h_0}. \tag{16}$$

The parameter β is a numerical constant for a given rubber, and its values have been tabulated for different hardness values of rubbers [22].

Thus, from equation (15) the elastic normal modulus depends upon three terms, the last one being the undeformed elastic normal modulus which varies with factors such as the frequency and temperature. The first two terms depend only on the geometry, since for a given rubber β is constant. Thus, the relationship between the compressed and undeformed moduli is dependent only on the geometry, for the same conditions.

Payne [14, 17–19] extended the analysis leading equation (15) to include the loss normal modulus, and proposed that complex instead of elastic moduli be used. Clearly, this argument implies that the loss factor must be constant, and generates the equation

$$E^*_D = (1 + \beta S^2)\left(\frac{2 + \lambda^3}{\lambda^3}\right) G^*_0. \tag{17}$$

Rubbers used for vibration isolators closely approximate incompressible elastic materials for which $\nu = 0{\cdot}5$ [22] and thus

$$E^*_0 = 3G^*_0 \tag{18}$$

which implies that equations (15) and (17) may respectively be expressed as

$$E'_D = (1 + \beta S^2)\left(\frac{2 + \lambda^3}{3\lambda^3}\right) E'_0 \tag{19}$$

and

$$E^*_D = (1 + \beta S^2)\left(\frac{2 + \lambda^3}{3\lambda^3}\right) E^*_0. \tag{20}$$

Note that the factor of 1/3 that appears in equations (19) and (20) originates in equation (18), which is an approximation that becomes less accurate as the hardness of the rubber increases. This is because the proportion of added non-rubber constituents increases and also because of thixotropic and other effects, and for hard rubbers the approximation may be taken as $E^* \approx 4G^*$ giving a factor of 1/4 instead of 1/3.

However, the factor of 1/3 is needed to ensure that equations (19) and (20) are valid for the undeformed case. If the rubber element is undeformed, then $\lambda = 1$ which upon substitution into equations (19) and (20) yields

$$E'_D = (1 + \beta S^2)E'_0 \tag{21}$$

and

$$E^*_D = (1 + \beta S^2)E^*_0. \tag{22}$$

Equations (21) and (22) are intuitively correct for the undeformed case, which implies that the factor of 1/3 should remain unchanged. Consequently, it is expected that the accuracy of equations (19) and (20) will diminish as the hardness of the rubber increases.

4.1. PREVIOUS RESEARCH

Previous researchers have investigated the effects of static extension [23–26] and compression [14, 18, 19, 27–36] on the loss factors of rubbers. Their findings indicate that in general, the loss factor is a function of the compression ratio, the elastic normal modulus is given by equation (21), and equation (22) is valid if the loss factor is constant over the range of static strains of concern. Equation (22) is also approximately true for rubbers that have low loss factors, such as unfilled rubbers, since the loss normal modulus is small compared to the elastic normal modulus. The cited experimental work has been conducted at frequencies up to approximately 400 Hz [28] and room temperatures of approximately 18–23°C.

The vibration isolators of primary concern are those that have elements of natural rubber vulcanisates filled with carbon black. Of the cited researchers, those that investigated these rubbers were Kosten [27], Vashchuk and Rosin [30], and Sullivan and Demery [25, 26]. Kosten [27] reported on the absolute value of the complex normal modulus, and Sullivan and Demery [25, 26] investigated the extensional case. In terms of the effect of the compression ratio, the results of Vashchuk and Rosin [30], and Klyukin [31] were unclear.

In summary, it may be said that the findings of previous researchers are not conclusive as regards the validity of equation (22). To be able to predict the effect of the compression ratio on the dynamic properties of vibrations isolators, it is assumed that equation (22) is approximately valid for natural rubber vulcanisates filled with carbon black under common vibration isolator conditions. This assumption will be treated as a starting point.

5. LONG COMPRESSED RUBBER ROD

Consider a long compressed rubber rod with compression ratio λ, and that is homogeneous, of uniform cross-section and right prismatic shape. Assume that it has phase velocity c_L^* and apparent complex normal modulus E_L^*. From the wave equation

$$c_L^* = \sqrt{\frac{E_L^*}{\rho}}. \tag{23}$$

Replacing E_R^* by E_L^* in equation (20) and combining equations (2), (20) and (23) yields

$$c_L^* = \left[\frac{(1+\beta S^2)(2+\lambda^3)}{3\lambda^3}\right]^{1/2} c_0^*. \tag{24}$$

6. SHORT COMPRESSED RUBBER ROD

Now include the lateral motion effects of a short rubber rod, discussed in section 3. Consider a short compressed rubber rod with compression ratio λ, and that is homogeneous, of uniform cross-section and right prismatic shape. Assume that it has phase velocity c_R^* and apparent complex normal modulus E_R^*. From the wave equation

$$c_R^* = \sqrt{\frac{E_R^*}{\rho}}. \tag{25}$$

Replacing c_L^* by c_R^*, and c_0^* by c_F^* in equation (24) gives

$$c_R^* = \left[\frac{(1+\beta S^2)(2+\lambda^3)}{3\lambda^3}\right]^{1/2} c_F^*. \tag{26}$$

Combining equations (6), (9) and (26) yields

$$c_R^* = \left[\frac{(1+\beta S^2)(2+\lambda^3)}{3\lambda^3}\right]^{1/2} \left[1 - \left(\frac{\omega v r_G}{c_0^*}\right)^2\right]^{1/2} c_0^*. \tag{27}$$

Define the phase velocity correction factor Ω_R^* such that equation (27) may be expressed in the form

$$c_R^* = \Omega_R^* c_0^*, \tag{28}$$

where

$$\Omega_R^* = \left[\frac{(1+\beta S^2)(2+\lambda^3)}{3\lambda^3}\right]^{1/2} \left[1 - \left(\frac{\omega v r_G}{c_0^*}\right)^2\right]^{1/2}. \tag{29}$$

The magnitude of the phase velocity correction factor is $\Omega_R = |\Omega_R^*|$. Then from equations (2), (25) and (28)

$$E_R^* = (\Omega_R^*)^2 E_0^*. \tag{30}$$

Alternatively, equations (9), (10) and (29) give

$$\Omega_R^* = \left[\frac{(1+\beta S^2)(2+\lambda^3)}{3\lambda^3}\right]^{1/2} \left[1 + \left(\frac{\omega v r_G}{c_R^*}\right)^2\right]^{-1/2}. \tag{31}$$

7. SHORT COMPRESSED RUBBER ROD WITH BARREL SHAPE

Equations (27)–(30) derived in sections 2–6, when applied to a vibration isolator, imply that the rubber element of the vibration isolator is of uniform shape and cross-sectional area, i.e., that it is not under static compression. To be able to apply these equations to a vibration isolator under static compression, the value for the complex normal modulus used in equation (20) needs to be corrected.

Assume that the deformation effects of the hydrostatic pressure within the rubber element caused by the static compression are approximately taken into account by the shape factor term $(1 + \beta S^2)$ in equation (20) [37, Appendix 1]. This term is included in the present discussion in equation (29). This is also known as the end effect and arises from the end plates being securely bonded to the ends of the rubber element. Of concern is the dynamic small stress strain behaviour, which is superposed on the static stress and strain. For strain amplitudes not greater than 1×10^{-3}, linear behaviour is assumed (see section 4).

Consider the deformed shape of the compressed rubber element of a vibration isolator that experiences sinusoidal vibration at the circular frequency ω. The longitudinal distance x along the rod is measured from one end (see Figure 2). Compressive stresses and strains are defined to be positive, so that a compressive stress produces a positive stress and strain. Let the longitudinal vibration of the rod result in a longitudinal displacement $u^* = u^*(x)$.

The analysis in sections 2–6 has assumed that the cross-sectional area remains constant, but in reality it is a function of the axial distance x, i.e., $A = A(x)$. To take this into account, Snowdon [4] developed a wave equation which when applied to the present situation gives

$$\frac{\partial^2 u^*}{\partial x^2} + \frac{1}{A}\frac{\partial A}{\partial x}\frac{\partial u^*}{\partial x} + \left(\frac{\omega}{c_R^*}\right)^2 u^* = 0. \tag{32}$$

By using the velocity c_R^* in equation (32) the corrections for radial inertia, compression and shape factor have been included. Knowledge of the function $A = A(x)$ means that equation (32) may be employed to predict the longitudinal behaviour.

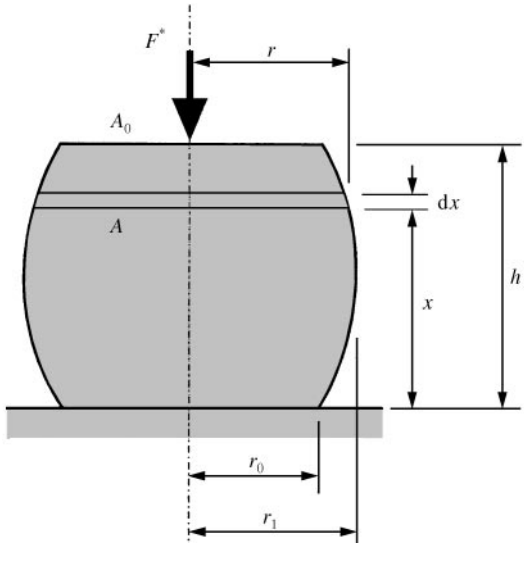

Figure 2. Deformed barrel shape of compressed cylindrical rubber element.

Assume that lateral plane sections of the rubber remain plane during the deformation of the vibration isolator. This implies that longitudinal sections of the rubber form parabolic shapes [37, Appendix 1]. Consider the external longitudinal surface shape of a compressed cylindrical rubber element of a vibration isolator (Figure 2). The rubber element has end radii of r_0, a central radius of r_1 and a height of h. Let a point on the surface have co-ordinates (r, x), where r is the radius at a longitudinal distance x from the bottom end plate. Then the locus of points satisfies a parabolic equation of the form

$$\left(x - \frac{h}{2}\right)^2 = 2p(r_1 - r), \tag{33}$$

where $2p$ is the latus rectum.

Substituting the boundary points of $(r_0, 0)$ and (r_0, h) into equation (33) yields the latus rectum and equation (33) becomes

$$r = r_1 - \left(\frac{2x}{h} - 1\right)^2 (r_1 - r_0). \tag{34}$$

From equation (34) the volume K of the rubber element is given by

$$K = \int_{x=0}^{x=h} \pi \left[r_1 - \left(\frac{2x}{h} - 1\right)^2 (r_1 - r_0) \right]^2 \mathrm{d}x, \tag{35}$$

which simplifies to

$$K = \frac{\pi h}{15} (3r_0^2 + 4r_0 r_1 + 8r_1^2). \tag{36}$$

The undeformed height of the rubber element is h_0, the undeformed cross-sectional area is A_0 and the compression ratio is λ. Let the undeformed volume be K_0. Then

$$A_0 = \pi r_0^2 \tag{37}$$

and

$$K_0 = h_0 A_0. \tag{38}$$

The compressed height is

$$h = \lambda h_0. \tag{39}$$

Assuming that the rubber is incompressible implies that $K = K_0$, which from equations (36)–(39) yields

$$8\xi^2 + 4\xi + 3\left(\frac{\lambda - 5}{\lambda}\right) = 0, \tag{40}$$

where

$$\xi = \frac{r_1}{r_0}. \tag{41}$$

Solving the quadratic equation (40) and selecting the positive root gives

$$\xi = \frac{1}{4}\left(\sqrt{5\left(\frac{6-\lambda}{\lambda}\right)} - 1\right). \tag{42}$$

The compression ratio may be expressed in terms of the static strain ε_S as

$$\lambda = 1 - \varepsilon_S, \tag{43}$$

which when substituted into equation (42) gives

$$\xi = \frac{1}{4}\left(5\left(1 + \frac{\varepsilon_S}{5}\right)^{1/2}(1-\varepsilon_S)^{-1/2} - 1\right). \tag{44}$$

The strain terms in equation (44) may be expanded using infinite binomial series. For small strains the expansions may be approximated by ignoring terms containing strains of order 2 and above, which yields the approximation

$$\xi = (1 + \tfrac{3}{4}\varepsilon_S). \tag{45}$$

Gent and Lindley [37, Appendix 1] considered the compression behaviour of a circular rubber element for small strains, and derived an equation that agrees with equation (45).

Substituting equations (42) and (41) into equation (34) gives

$$r = \frac{r_0}{4}\left[\sqrt{5\left(\frac{6-\lambda}{\lambda}\right)} - \left(\frac{2x}{h} - 1\right)^2\left(\sqrt{5\left(\frac{6-\lambda}{\lambda}\right)} - 5\right) - 1\right]. \tag{46}$$

The cross-sectional area A is given by

$$A = \pi r^2. \tag{47}$$

Substituting equation (46) into equation (47) yields

$$A = \frac{\pi r_0^2}{8}\left\{\begin{array}{l} 5\left[\left(\frac{3+2\lambda}{\lambda}\right) - \sqrt{5\left(\frac{6-\lambda}{\lambda}\right)}\right]\left(\frac{2x}{h} - 1\right)^4 - 6\left[\left(\frac{5}{\lambda}\right) - \sqrt{5\left(\frac{6-\lambda}{\lambda}\right)}\right]\left(\frac{2x}{h} - 1\right)^2 \\ \quad + \left[\left(\frac{15-2\lambda}{\lambda}\right) - \sqrt{5\left(\frac{6-\lambda}{\lambda}\right)}\right] \end{array}\right\}. \tag{48}$$

Therefore from equation (48),

$$\frac{\partial A}{\partial x} = \frac{\pi r_0^2}{h}\left(\frac{2x}{h} - 1\right)\left\{5\left[\left(\frac{3+2\lambda}{\lambda}\right) - \sqrt{5\left(\frac{6-\lambda}{\lambda}\right)}\right]\left(\frac{2x}{h} - 1\right)^2 - 3\left[\left(\frac{5}{\lambda}\right) - \sqrt{5\left(\frac{6-\lambda}{\lambda}\right)}\right]\right\}. \tag{49}$$

Substituting equations (48) and (49) into equation (32) yields the partial differential equation

$$\frac{\partial^2 u^*}{\partial x^2} + \frac{\partial u^*}{\partial x} f_1 + k^{*2} u^* = 0, \tag{50}$$

where f_1 is a function of λ and x/h, defined as

$$f_1 = \frac{1}{A}\frac{\partial A}{\partial x} \tag{51}$$

with A and $\partial A/\partial x$ given by equations (48) and (49), and

$$k^* = \frac{2\pi}{\Lambda_R^*}. \tag{52}$$

The wave number is $k = |k^*|$ and the wavelength is $\Lambda_R = |\Lambda_R^*|$.

Equation (50) does not have a closed-form solution, and so numerical solutions are determined in section 7.1.1 and an approximate algebraic solution is proposed in section 7.2.

7.1.1. *Numerical solution*

Numerical solutions of equation (50) for compression ratios of 0·9, 0·85, 0·8, 0·75 and 0·7 were determined using Matlab [38], and the procedure used for each solution is as follows. The quantities k^* and Λ_R^* are assumed to be real.

Equation (50) was solved using increments of $\Delta x = 0{\cdot}0001h$ from $x = 0$ to h, with boundary conditions of $u^* = 0$ at $x = 0$ and h. At time t, the solution has the form

$$u^* = U_0 U \sin(kx) e^{j\omega t} \tag{53}$$

where

$$k = \frac{2\pi}{\Lambda_R}, \tag{54}$$

U_0 is a constant and the variable U is a function of x/h, with $U = 1$ at $x/h = 0$ and 1. U represents the geometrical effect of deforming the cylindrical rubber element on the amplitude of the wave. The equation of the undeformed rubber element is given by equation (53) with $U = 1$. Define the spatial variable u_1 to be a function of x/h by

$$u_1 = U \sin\left[kh\left(\frac{x}{h}\right)\right]. \tag{55}$$

To discern the amplitude envelope of u_1, the height of the rubber element was set at 200 cycles of the wave with $\Lambda_R = 0{\cdot}005h$. This yielded u_1, using equations (54) and (55), as

$$u_1 = U \sin\left[400\pi\left(\frac{x}{h}\right)\right]. \tag{56}$$

U was then determined by applying the Hilbert transform to u_1, and a polynomial of order 4 was fitted to the data points of U.

From the work of Love [5], Abramson *et al.* [3] and Skudrzyk [6], the phase velocity reduction factor of Love is given by considering the kinetic energy of the vibrating rod, as follows up to equation (60). All quantities are considered to be real. The kinetic energy of the rod excluding the lateral motion T_1 is given by

$$T_1 = \left|\frac{\rho A}{2}\int_0^h \left(\frac{\partial u^*}{\partial t}\right)^2 \mathrm{d}x\right| \tag{57}$$

and the kinetic energy of the rod due only to the lateral motion T_2 is given by

$$T_2 = \left| \frac{\rho A}{4} \int_0^h \left(\frac{vr\partial^2 u^*}{\partial x \partial t} \right)^2 \mathrm{d}x \right|. \tag{58}$$

Therefore, the increase in the total kinetic energy due to the lateral motion is

$$\alpha = 1 + \frac{T_2}{T_1}. \tag{59}$$

The potential energy is unaffected by the lateral motion. The increase in kinetic energy may be accounted for by increasing the density of the rod by the factor α, which in equation (25) implies a phase velocity reduction factor Θ_K of

$$\Theta_K = \frac{1}{\sqrt{\alpha}}. \tag{60}$$

Equations (53) and (57)–(60) with the specified boundary conditions of the second paragraph of this section yield

$$\Theta_K = \left[1 + \frac{v^2 \int_0^h r^2 \left(\dfrac{\partial U}{U \partial x} \sin(kx) + k \cos(kx) \right)^2 \mathrm{d}x}{2 \displaystyle\int_0^h U^2 \sin^2(kx)\, \mathrm{d}x} \right]^{-1/2}. \tag{61}$$

For constant U and r, equation (61) with equations (8) and (54) reduces to the same form expressed by equation (10), as expected. To enable a meaningful comparison to be made later in section 7.2.5, define the diameter-to-wavelength ratio X_R as

$$X_R = \frac{2r_0}{\Lambda_R \sqrt{\lambda}}. \tag{62}$$

For the purposes of computation, the values of $h_0 = 1$ and $r_0 = 0{\cdot}1$ were selected. Therefore $h = \lambda$ from equation (39), and for a given diameter-to-wavelength ratio, equation (62) gives Λ_R. It is assumed that $v = 0{\cdot}5$. Thus, the numerical values of Θ_K were determined from the values of r, k and the polynomial fit of U using equations (46), (54) and (61).

The curves of Θ_K against X_R are plotted in Figure 3, for the compression ratios considered. The other curves shown in the figure are derived in section 7.2.5.

7.2. PROPOSED CORRECTION FOR BARREL SHAPE

An approximate closed-form solution is proposed and compared with the numerical solutions of section 7.1.1. This solution approximates the compressed barrel of the rubber element with a regular right cylinder of equal height and volume, termed the effective cylinder. It is assumed that the rubber volume remains unchanged during deformation, and that the end effects are taken into account by the shape factor term $(1 + \beta S^2)$, as stated in section 7. The proposed solution also accounts for the strain in determining the complex normal modulus referenced to the compressed state. In sections 7.2.1–7.2.5, the cross-sectional areas and the radii of gyration for the effective cylinder and barrel are determined and compared.

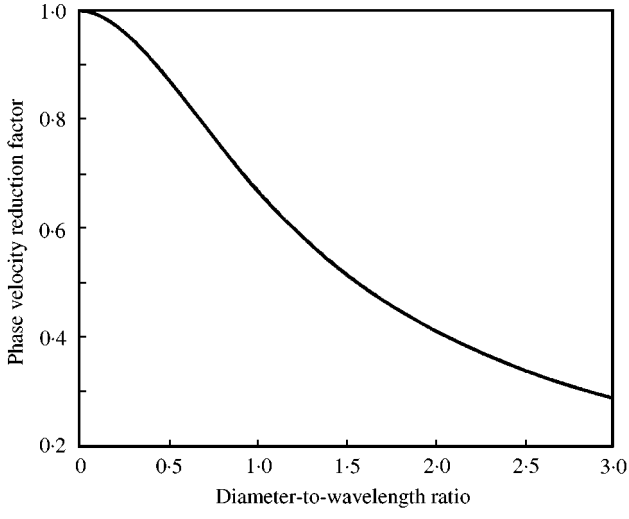

Figure 3. Magnitude of phase velocity reduction factor for compressed rubber element based on the Love theory and proposed effective rubber cylinder. Values for compression ratios of 0·95, 0·9, 0·85, 0·8, 0·75 and 0·7 are shown, but are indistinguishable from each other on this scale.

7.2.1. *Cross-sectional area of effective cylinder*

Consider the notion of an effective cross-sectional area of the barrelled rubber element of the vibration isolator. Clearly, for a large compression ratio λ, the cross-sectional area varies for a symmetrical vibration isolator from a fixed value at the bonded ends to a maximum value midway between the ends. The effective cross-sectional area has a value that lies between the areas of the bonded ends and the area at the centre. Define the effective cross-sectional area to be the cross-sectional area of the effective cylinder. Correspondingly, the true stress will vary as a function of the height. Consequently, the effective stress is defined to be the stress that corresponds to the effective cross-sectional area.

The undeformed element has height h_0 and cross-sectional area A_0, and the effective cylinder has height h and cross-sectional area A_C. The barrelled and effective cylindrical elements have complex normal moduli of E_D^* and E_C^* respectively. The modulus E_C^* is an apparent complex normal modulus defined for the purpose of applying the wave equation. For a given compression ratio, the area A_C is equal to the uniform cross-sectional area of the compressed rubber with unbonded ends at the same compression ratio. Assuming that the volume of the rubber remains constant,

$$A_C = \frac{A_0}{\lambda}. \tag{63}$$

7.2.2. *Radius of gyration of effective cylinder*

Consider a rubber element of regular right cylindrical shape and effective cross-sectional area A_C. This is the effective rubber cylinder, and its radius r_C is given by equations (47) and (63) as

$$r_C = \frac{r_0}{\sqrt{\lambda}}. \tag{64}$$

Therefore, from equations (8) and (64), the radius of gyration r_G is given by

$$r_G = a_C r_0 \tag{65}$$

where

$$a_C = \frac{1}{\sqrt{2\lambda}}. \tag{66}$$

7.2.3. *Cross-sectional area of barrel*

Consider the cylindrical elemental volume at height x of the barrel (see Figure 2). It has height $\mathrm{d}x$, cross-sectional area A, radius r and longitudinal displacement $\mathrm{d}u^*$ when an exciting force F^* is applied to the end of the compressed element. Therefore

$$u^* = \frac{F^*}{E_D^*} \int_{x=0}^{x=h} \frac{\mathrm{d}x}{A}. \tag{67}$$

It is desired to find the cross-sectional area A_E of an equivalent cylinder, that gives the same longitudinal displacement of the compressed element at the same compression ratio. For a regular right cylinder, equation (67) gives

$$u^* = \frac{F^* h}{E_D^* A_E}. \tag{68}$$

Solving for A_E from equations (67) and (68) gives

$$A_E = h \left(\int_{x=0}^{x=h} \frac{\mathrm{d}x}{A} \right)^{-1}. \tag{69}$$

From equations (47) and (69),

$$A_E = \pi h \left(\int_{x=0}^{x=h} \frac{\mathrm{d}x}{r^2} \right)^{-1}. \tag{70}$$

Let the integration term in equation (70) be I, which from equation (34) is given by

$$I = \int_{x=0}^{x=h} \frac{\mathrm{d}x}{[r_1 - (2x/h - 1)^2 (r_1 - r_0)]^2}. \tag{71}$$

Let the variable s be defined by

$$s = \frac{2x}{h} - 1 \tag{72}$$

and the parameter a by

$$a = \sqrt{\frac{r_1}{r_1 - r_0}} \tag{73}$$

for $r_1 \neq r_0$.

Then equation (71) may be written in the more convenient form of

$$I = \frac{h}{2(r_1 - r_0)^2} \int_{s=-1}^{s=1} \frac{\mathrm{d}s}{(a^2 - s^2)^2}. \tag{74}$$

Performing the definite integration of equation (74) gives

$$I = \frac{h}{2r_0^2 \xi} \left[1 + \frac{\ln[2\xi - 1 + 2\sqrt{\xi(\xi - 1)}]}{2\sqrt{\xi(\xi - 1)}} \right] \tag{75}$$

where ξ is defined by equation (41) and given by equation (42).

Substituting equation (75) into equation (70) with equation (37) yields an equivalent cylinder factor E as

$$A_E = \mathrm{E} A_0, \tag{76}$$

where

$$\mathrm{E} = \frac{4\xi\sqrt{\xi(\xi - 1)}}{2\sqrt{\xi(\xi - 1)} + \ln[2\xi - 1 + 2\sqrt{\xi(\xi - 1)}]}. \tag{77}$$

7.2.4. *Radius of gyration of barrel*

From equation (7), the radius of gyration r_G of the rubber barrel is given by

$$r_G^2 = \frac{1}{2h} \int_{x=0}^{x=h} r^2 \, \mathrm{d}x. \tag{78}$$

Substituting equation (46) into equation (78) gives

$$r_G^2 = \frac{r_0^2}{32h} \int_{x=0}^{x=h} \left[\sqrt{5\left(\frac{6 - \lambda}{\lambda}\right)} - \left(\frac{2x}{h} - 1\right)^2 \left(\sqrt{5\left(\frac{6 - \lambda}{\lambda}\right)} - 5 \right) - 1 \right]^2 \mathrm{d}x. \tag{79}$$

Simplifying equation (79) produces

$$r_G = a_G r_0, \tag{80}$$

where

$$a_G = \frac{1}{\sqrt{2\lambda}}. \tag{81}$$

7.2.5. *Comparison of effective cylinder and barrel*

The two factors, $1/\lambda$ and E, for the cross-sectional area of an equivalent regular cylinder are compared in Table 1 over the range of compression ratios from 0·95 to 0·7. Note that equation (77) is not valid for a compression ratio of unity. The table also shows the percentage error of the $1/\lambda$ factor relative to E.

Vibration isolators are commonly used over the range of compression ratios from 0·95 to 0·80, and over this range the percentage difference between the two factors, $1/\lambda$ and E, is less than 1% (see Table 1). It is considered that the error introduced by using the factor $1/\lambda$ is acceptable. Therefore, the algebraically simpler factor $1/\lambda$ will be used instead of E in section 7.2.6.

TABLE 1

Factors for cross-sectional area

λ	$\frac{1}{\lambda}$	ξ	E	Difference (%)
0·95	1·053	1·039	1·052	0·05
0·90	1·111	1·081	1·109	0·21
0·85	1·177	1·126	1·171	0·49
0·80	1·250	1·175	1·239	0·91
0·75	1·333	1·229	1·131	1·48
0·70	1·429	1·288	1·398	2·22

The two factors, a_C and a_G for the radius of gyration of an equivalent regular cylinder are identical, equations (66) and (81). Therefore, the factor $1/\sqrt{2\lambda}$ will be used in section 7.2.6.

The two factors $1/\lambda$ and $1/\sqrt{2\lambda}$ respectively affect the apparent complex normal modulus and radius of gyration of the rod. Equation (61) does not take into account changes in the complex normal modulus, and so to compare its predictions to that of the effective cylinder, only the modified radius of gyration is included to give the reduced phase velocity correction factor of the effective cylinder Θ_B. All quantities are treated as real. Equations (4), (5), (10), (64) and (80) yield

$$\Theta_B = [1 + \tfrac{1}{2}(\pi v X_F)^2]^{-1/2} \tag{82}$$

where the diameter-to-wavelength ratio X_F is defined by

$$X_F = \frac{2r_0}{\Lambda_F\sqrt{\lambda}}. \tag{83}$$

For equal wavelengths $\Lambda_F = \Lambda_R$, equations (62) and (83) imply that $X_F = X_R$. Thus the curves of Θ_B against X_F are also plotted in Figure 2, for the compression ratios of 0·9, 0·85, 0·8, 0·75 and 0·7. The Θ_B and Θ_K curves of Figure 3 show close agreement, and for diameter-to-wavelength ratios from 0 to 3 agree within 1% of each other, referenced to the Θ_K values.

This gives high confidence in the proposed effective rubber cylinder as a model for the barrel shape of the deformed rubber element.

7.2.6. *Proposed correction factor*

Consider the effective rubber cylinder with the correction factors derived in the previous sections 7.2.1–7.2.5, namely $1/\lambda$ for the cross-sectional area and $1/\sqrt{2\lambda}$ for the radius of gyration. Let the stress of the effective rubber cylinder be σ_C^*, and the compressed stress calculated with the area of the bonded ends be σ^*. Therefore from equation (63),

$$\sigma_C^* = \lambda\sigma^*. \tag{84}$$

The compressed strain ε^* relative to the undeformed area and height was used in sections 2–6. However, in equation (32) the compressed condition is treated as the reference state. Let the compressed strain with respect to the compressed height be ε_C^* for the effective

rubber cylinder. Therefore

$$\varepsilon_C^* = \frac{\varepsilon^*}{\lambda}. \tag{85}$$

The effective cylinder has a complex normal modulus E_C^*, which corresponds to σ_C^* ad ε_C^*, and the complex normal modulus corresponding to σ^* and ε^* is E_R^*. From equations (84) and (85), E_C^* is given by

$$E_C^* = \lambda^2 E_R^*. \tag{86}$$

Let Ω_C^* be the phase velocity correction factor and c_C^* the phase velocity of the effective rubber cylinder of modulus E_C^*. Then

$$E_C^* = (\Omega_C^*)^2 E_0^*. \tag{87}$$

and

$$c_C^* = \Omega_C^* c_0^*. \tag{88}$$

Applying the correction of equation (86) to equation (30) gives

$$E_C^* = (\lambda \Omega_R^*)^2 E_0^* \tag{89}$$

Comparing equations (87) and (89) yields

$$\Omega_C^* = \lambda \Omega_R^* \tag{90}$$

and from equations (11) and (28), Ω_C^* may be written as

$$\Omega_C^* = \Omega_C e^{j\psi/2}. \tag{91}$$

The magnitude of the phase velocity of the effective rubber cylinder is $c_c = |c_c^*|$, and equations (3) and (88) give

$$c_C^* = c_C e^{j(\delta_0 + \psi)/2}. \tag{92}$$

From equations (29), (88) and (90)

$$c_C^* = \left\{ \frac{(1 + \beta S^2)(2 + \lambda^3)[(c_0^*)^2 - (\omega v r_G)^2]}{3\lambda} \right\}^{1/2}. \tag{93}$$

Applying equation (65) with a Poisson ratio of 0·5 simplifies equation (93) to

$$c_C^* = \frac{\{(1 + \beta S^2)(2 + \lambda^3)[8\lambda(c_0^*)^2 - (\omega r_0)^2]\}^{1/2}}{2\sqrt{6}\lambda}. \tag{94}$$

Alternatively, from equations (31) and (90)

$$\Omega_C^* = \left[\frac{(1 + \beta S^2)(2 + \lambda^3)}{3\lambda} \right]^{1/2} \left[1 + \left(\frac{\omega v r_G}{c_C^*} \right)^2 \right]^{-1/2}, \tag{95}$$

where r_G is given by equation (65).

Let the wavelength and frequency of the longitudinal wave in the effective rubber cylinder be Λ_C and f respectively. Then

$$c_C = f\Lambda_C. \tag{96}$$

Combining equations (4), (92), (95) and (96) gives the magnitude Ω_C of the phase velocity correction factor as

$$\Omega_C = \left[\left(\frac{2\pi v r_G}{\Lambda_C}\right)^4 + 2\left(\frac{2\pi v r_G}{\Lambda_C}\right)^2 \cos(\delta_0 + \psi) + 1\right]^{-1/4} \left[\frac{(1+\beta S^2)(2+\lambda^3)}{3\lambda}\right]^{1/2}, \tag{97}$$

where ψ is given by equation (12) and r_G is given by equation (65).

Using a Poisson ratio of 0·5 in equation (97) and substituting equation (65) gives

$$\Omega_C = \sqrt{\frac{2}{3}}\Lambda_C[(\pi r_0)^4 + 4\lambda(\pi r_0 \Lambda_C)^2 \cos(\delta_0 + \psi) + 4\lambda^2\Lambda_C^4]^{-1/4}(1+\beta S^2)^{1/2}(2+\lambda^3)^{1/2}, \tag{98}$$

where

$$\psi = \tan^{-1}\left[\frac{(\omega r_0)^2 \sin\delta_0}{8\lambda c_0^2 - (\omega r_0)^2 \cos\delta_0}\right]. \tag{99}$$

Equations (65), (93) and (94) embody correction factors for the static compressive effects on the phase velocity of longitudinal-wave propagation in a short rubber rod compressed to a barrel shape. The individual factors have been proposed by previous researchers, but a literature search showed that they have not been combined and applied to rubber rods under static compression using the notion of an effective rubber cylinder to account for the barrelling. These equations are proposed by this study.

From section 3.1 an upper limit needs to be set on the diameter-to-wavelength ratio. Assume that the error analysis of section 3.1 may be applied by using the effective rubber cylinder to account for the barrelling. Let the maximum tolerable error in the phase velocity reduction factor be 10%. Then the maximum diameter-to-wavelength ratio is 1·41, where the diameter is that of the effective rubber cylinder.

7.2.7. *Comparison of proposed correction factor and experimental data*

This section compares experimental data from previous research with predictions based on this study. For this comparison it is necessary to use equation (98), which is in terms of the wavelength Λ_C of the longitudinal wave in the effective rubber cylinder.

Morris *et al.* [28] investigated the dynamic properties of rubber using a modified bar transmission method developed from the strip transmission, or longitudinal wave resonance method described by Nolle [39]. They measured the longitudinal wave velocity of a cylindrical rubber specimen under static compression, by determining its longitudinal resonant frequency. The specimen was made of an unfilled natural rubber vulcanisate of undeformed dimensions 19·05 mm diameter × 70·5 mm height, and loss factor 0·15.

Initially, the effect of bearing friction on the resonant frequency was investigated and found to be nil, and the subsequent tests were conducted using silicone grease at the ends of the specimens. This end effect is accounted for by the term $\sqrt{1+\beta S^2}$ in equation (98). At a compression strain of 0·018 the measured elastic normal modulus was 2·06 MPa and the loss factor was 0·15. Using this value of 2·06 MPa for the static normal modulus, the interpolated value for β is 1·50 [22]. From equation (16) the value of S is 0·0676, using

$r_0 = 9{\cdot}525 \times 10^{-3}$ and $h_0 = 7{\cdot}055 \times 10^{-2}$ m. Therefore, the value of $\sqrt{1 + \beta S^2}$ is 1·003, which represent 0·3% difference between the extreme cases of unbonded and bonded ends. Therefore, the measured result of negligible difference is expected. Thus, equation (98) still remains applicable with $S = 0$ to take into account the rubber ends being lubricated and not bonded.

The experimental results obtained [28] are given in Table 2, which at different values of the compression ratio λ and wavelength Λ_C, lists the measured values of the longitudinal resonant frequency f_M. The measured wavelength is set equal to Λ_C. For the test set-up used, the wavelength was equal to twice the length of the compressed rubber specimen [28], which gave Λ_C. The loss factor was approximately constant ranging from 0·15 to 0·16, and so there should be very little phase error introduced by using equation (98). Loss factors of 0·15 and 0·16 correspond to loss angles 8·5 and 9·1°. The radius of gyration was calculated from equation (65) using $r_0 = 9{\cdot}525 \times 10^{-3}$ m.

Assume that the undeformed long rod velocity is 46·2 m/s, which is the measured long rod velocity at 1·8% compressive strain. This measurement was conducted at the minimum experimental deformation of the sample. Table 2 also lists the predicted values of the resonant frequency f_C, calculated as follows.

An iterative solution using the Jacobian method with the numeric computation Matlab software [38] was employed. For a given frequency f_C, equation (99) calculates the value of ψ using $\delta_0 = 8{\cdot}53°$, $c_0 = 46{\cdot}2$ m/s and $\omega = 2\pi f_C$. From equation (98) the magnitude Ω_C of the phase velocity correction factor was calculated from the known parametric values and by putting $S = 0$. Then from equation (88) the magnitude c_C of the phase velocity was determined as

$$c_C = \Omega_C c_0. \tag{100}$$

Therefore, the resonant frequency of the effective rubber cylinder f_C was calculated from

$$f_C = \frac{c_C}{\Lambda_C}. \tag{101}$$

This value of f_C was compared with the starting value and iterated to give the solved value. The percentage error between the measured and predicted longitudinal resonant frequencies, i.e., f_M and f_C respectively, is listed in the last column.

The maximum value of the diameter-to-wavelength ratio is 0·01905/0·1168 = 0·163. From section 3.1, the error in the calculated short rod velocity does not exceed 4% for diameter-to-wavelength ratios from 0 to 1·20 for a rod of constant cross-sectional area and negligible loss factor. Since the maximum value of the diameter-to-wavelength ratio is much

TABLE 2

Determination of longitudinal resonant frequencies

λ	Λ_C (m)	f_M (Hz)	Ω_C	c_C (m/s)	f_C (Hz)	Error (%)
0·982	0·1385	327	0·9886	45·67	329·8	0·8
0·936	0·1321	346	0·9888	45·68	345·8	0·0
0·900	0·1270	359	0·9904	45·76	360·3	0·4
0·864	0·1219	385	0·9932	45·89	376·4	2·2
0·828	0·1168	405	0·9974	46·08	394·5	2·6

smaller than 1·20, it is reasonable to assume that equation (98) is not restricted by this parameter.

The precision of reproducibility of the resonant frequency f_M is given as 8 in 330 Hz [28], i.e., 2·4%. As can be seen from Table 2, the predicted resonant frequency f_C is within this error band except for the maximum compression case, which has a marginally higher error. In addition, there must have been measurement errors that were not specified. Therefore, for this case the predicted resonant frequency based on equation (98) agrees satisfactorily with the experimental values.

The ends were lubricated during the test to improve the contact with the transducers, and not to specifically reduce the friction. It may be assumed that the specimen compressed to a shape somewhere between the effective cylinder and the barrel with fixed ends. The analysis of this section gives confidence in the application of the proposed equations (93) and (94).

8. CONCLUSIONS

Longitudinal wave equations for a short rod were developed by Love [5], and were applied by Snowdon [4] to the rubber element of a vibration isolator. Gent and Lindley [37] showed that the compressed rubber element assumes a parabolic shape.

Based on the work of Snowdon [4], and Gent and Lindley [37], wave equations have been derived for the barrel shape of the deformed rubber element of a vibration isolator under static compression. The wave equations include a partial differential equation, and do not have a closed-form solution. Consequently, an approximate algebraic solution was proposed in terms of the effective rubber cylinder and the compression ratio. The predictions of the effective rubber cylinder agreed well with numerical solutions of the wave equations for the deformed rubber element.

Payne [14] proposed the relationship between the complex normal modulus of the rubber element of a vibration isolator under static compression, and its compression ratio. The work of Payne was combined with the proposed model of an effective rubber cylinder, to account for the effect of static compression on the apparent complex normal modulus of a compressed rubber. Of interest were natural rubber vulcanisates filled with carbon black. This gave equations (93) and (94), and the latter was expressed as the magnitude equation (98). Predictions using the proposed equation (98) agreed with experimental data of Morris *et al.* [28].

Equations (93) and (94) embody correction factors for the static compressive effects on the phase velocity of longitudinal wave propagation in a short rubber rod compressed to a barrel shape. The individual factors have been proposed by previous researchers, but a literature search showed that they have not been combined and applied to rubber rods under static compression using the notion of an effective rubber cylinder to account for the barrelling.

The author has undertaken experimental work [40] and consequently proposed modifications to equations (93) and (94) that improve their accuracy. This work is reported in a companion paper [41].

ACKNOWLEDGMENT

The author gratefully acknowledge Dr Chris Norwood, Maritime Platforms Division, DSTO, and Dr Hugh Williamson from the University of New South Wales, for discussions

on themes of this paper. He also appreciates the support of AMRL during this study, as part of the work for a Ph.D. from the University of New South Wales.

REFERENCES

1. J. C. SNOWDON 1979 *Journal of the Acoustical Society of America* **66**, 1245–1274. Vibration isolation: use and characterisation.
2. C. H. HANSEN and S. D. SNYDER 1997 *Active Control of Noise and Vibration*. London: E & FN Spon.
3. H. N. ABRAMSON, H. J. PLASS and E. A. RIPPERGER 1958 *Advanced Applied Mechanics* **5**, 11–194. Stress wave propagation in rods and beams.
4. J. C. SNOWDON 1968 *Vibration and Shock in Damped Mechanical Systems*. New York: John Wiley & Sons.
5. A. E. H. LOVE 1959 *The Mathematical Theory of Elasticity*. London: Cambridge University Press, fourth edition.
6. E. SKUDRZYK 1968 *Simple and Complex Vibratory Systems*. Philadelphia: Pennsylvania State University Press.
7. L. POCHHAMMER 1876 *Journal fur die Reine und Angewandte Mathematik* (*Crelle's Journal*), (*translated as*: *Journal for Pure and Applied Mathematics*) **81**, 324–336. (Original in German). Uber die fortpflanzungsgeschwindigkeiten kleiner schwingungen in einem unbegrenzten isotropen kreiszylinder (translated as: About the propagation velocity of small vibrations in an infinite isotropic circular cylinder).
8. C. CHREE 1889 *Transactions of the Cambridge Philosophical Society* **14**, 250–369. The equations of an isotropic elastic solid in polar and cylindrical coordinates, their solutions and applications.
9. M. REDWOOD 1960 *Mechanical Waveguides*. London: Pergamon Press.
10. A. B. DAVEY and A.R. PAYNE 1964 *Rubber in Engineering Practice*. London: MacLaren & Sons.
11. D. BANCROFT 1941 *Physical Review* **59**, 588–593. The velocity of longitudinal waves in cylindrical bars.
12. A. R. PAYNE 1956 *Journal of Applied Polymer Science* **33**, 432. A note on the existence of a yield point in the dynamic modulus of loaded vulcanizates.
13. A. R. PAYNE and J. R. SCOTT 1960 *Engineering Design with Rubber*. London: MacLaren & Sons.
14. A. R. PAYNE 1957 *Research Association of British Rubber Manufacturers Research Report* 84, *Shawbury*. Dynamic properties of vulcanised rubber: 5, shape factors and functions in rubber engineering.
15. A. R. PAYNE 1955 *Research Association of British Rubber Manufacturers Research Report* R404, *Shawbury*. Dynamic properties of vulcanised rubber: 2, static and dynamic compression stress–strain curves for a pure gum natural rubber.
16. A. R. PAYNE 1955 *Research Association of British Rubber Manufacturers Research Report* IBC/427, *Shawbury*. Dynamic properties of vulcanised rubber: 3, review and extension of shape factor theories.
17. A. R. PAYNE 1956 *Nature* **177**, 1174–1175. Effect of shape on the static and dynamic stress–strain relationship of bonded rubber in compression.
18. A. R. PAYNE 1956 *Research Association of British Rubber Manufacturers Research Report* 77, *Shawbury*. Dynamic properties of vulcanised rubber: 4, shape factor theories.
19. A. R. PAYNE 1959 *The Engineer* **207**, 328–333, 368–370. Shape factors and functions in rubber engineering.
20. W. C. KEYS 1937 *Mechanical Engineering* **59**, 345–349. Rubber springs.
21. E. G. KIMMICH 1940 *India Rubber World* **103**, 45–50. Rubber in compression.
22. P. B. LINDLEY 1964 *Malaysian Rubber Producers' Research Association NR Technical Bulletin*, *Hertfordsire*. Engineering design with natural rubber.
23. A. W. NOLLE 1950 *Journal of Polymer Science* **5**, 1–54. Dynamic mechanical properties of rubberlike materials.
24. E. A. MEINECKE and M. I. TAFTAF 1983 *Proceedings of 124th Meeting of Rubber Division, American Chemical Society, Houston, TX*, 25–28 *October*, *Paper no*. 47. The influence of static deformations and carbon black loading on the dynamic properties of elastomers, Part I: extension.
25. J. L. SULLIVAN and V. C. DEMERY 1982 *Journal of Polymer Science*: *Polymer Physics Edition* **20**, 2083–2101. The nonlinear behavior of a carbon-black-filled elastomer.

26. J. L. SULLIVAN 1983 *Journal of Applied Polymer Science* **28**, 1993–2003. Viscoelastic properties of a gum vulcanizate at large static deformations.
27. C. W. KOSTEN 1939 *Rubber Chemistry and Technology* **12**, 381–393. Static and dynamic properties of rubber under compression.
28. R. E. MORRIS, R. R. JAMES and C. W. GUTTON 1956 *Rubber Chemistry and Technology* **29**, 838–851. A new method for determining the dynamic mechanical properties of rubber.
29. R. DE MARIE 1969 *Proceedings of 10th International Machine Tool Design and Research Conference, Manchester, September*, 83–93. Damping capacity of rubberlike materials loaded in compression, and dependence of their damping capacity on several parameters.
30. D. B. VASHCHUK and G. S ROSIN 1973 *Soviet Physics – Acoustics* **19**, 101–102. Dynamic properties of rubber.
31. I. I. KLYUKIN 1979 *Soviet Physics – Acoustics* **25**, 181–191. Vibration attenuation of resilient mounts and dampers underneath actively vibrating machines (review).
32. M. I. TAFTAF and E. A. MEINECKE 1983 *Proceedings of 124th Meeting of Rubber Division, American Chemical Society, Houston, TX*, 25–28 *October, Paper no.* 47. The influence of static deformations and carbon black loading on the dynamic properties of elastomers, Part II: compression.
33. R. T. M. FRASER, E. T. CLOTHIER and A. E. RAE 1984 *Admiralty Marine Technology Establishment Report* TM 84304, *Houlton Health*. The effect of shape factor on the loss tangent of viscoelastic pads.
34. P. BANDEL, G. P. GIULIANI and A. VOLPI 1986 *Kautschuk und Gummi Kunststoffe* **39**, 793–799. Analysis of the dynamic properties of rubber compounds and cord-rubber composites in tyres.
35. J. HARRIS and A. STEVENSON 1987 *International Journal of Vehicle Design* **8**, 553–576. On the role of non-linearity in the dynamic behaviour of rubber components.
36. O. NUUTILA, K. SAINE and H. TIENHAARA 1994 *Proceedings of 12th International Modal Analysis Conference, Honolulu*, 31 *January*–3 *February*, Vol. **2**, 1527–1532. The effect of non-linearities of rubber elements on the behavior of resilient mounting system.
37. A. N. GENT and P. B. LINDLEY 1959 *Proceedings of Institution of Mechanical Engineer* **173**, 111–122. The compression of bonded rubber blocks.
38. MATLAB 1996 *Matrix Laboratory Language for Technical Computing*, version 5.2. Natick, MA: The Maths Works.
39. A. W. NOLLE 1948 *Journal of Applied Physics* **19**, 753–774. Methods for measuring dynamic mechanical properties of rubber-like materials.
40. J. D. DICKENS 1998 *Ph.D. thesis, University of New South Wales, Canberra*. Dynamic characterisation of vibration isolators.
41. J. D. DICKENS in press *Journal of Sound and Vibration*. Dynamic model of vibration isolator under static load.